https://doi.org/10.5194/amt-2021-59
Preprint. Discussion started: 8 March 2021

Atmospheric Measurement Techniques Discussions

Efficacy of a portable, moderate-resolution, fast-scanning DMA for ambient aerosol size distribution measurements

Stavros Amanatidis[1,2], Yuanlong Huang[1], Buddhi Pushpawela[1], Benjamin C. Schulze[1], Christopher M. Kenseth[1], Ryan X. Ward[1], John H. Seinfeld[1], Susanne V. Hering[2], and Richard C. Flagan[1,*]

[1]California Institute of Technology, Pasadena, CA, USA
[2]Aerosol Dynamics Inc., Berkeley, CA, USA

Correspondence: Richard C. Flagan (flagan@caltech.edu)

Abstract.

Ambient aerosol size distributions obtained with a compact, scanning mobility analyzer, the "Spider" DMA, are compared to those obtained with a conventional mobility analyzer, with specific attention to the effect of mobility resolution on the measured size distribution parameters. The Spider is a 12-cm diameter radial differential mobility analyzer that spans the 10–500 nm size range with 30s mobility scans. It achieves its compact size by operating at a nominal mobility resolution $R = 3$ (sheath flow = 0.9 L/min, aerosol flow = 0.3 L/min), in place of the higher sheath-to-aerosol flow commonly used. The question addressed here is whether the lower resolution is sufficient to capture the dynamics and key characteristics of ambient aerosol size distributions. The Spider, operated at $R = 3$ with 30s up and down scans, was collocated with a TSI 3081 long-column mobility analyzer, operated at $R = 10$ with a 360s sampling duty cycle. Ambient aerosol data were collected over 26 consecutive days of continuous operation, in Pasadena, CA. Over the 20-500 nm size range, the two instruments exhibit excellent correlation in the total particle number concentrations and geometric mean diameters, with regression slopes of 1.13 and 1.00, respectively. Our results suggest that particle sizing at a lower resolution than typically employed is sufficient in obtaining the key properties of ambient size distributions.

1 Introduction

Mobility measurements of atmospheric aerosols in the 10–500 nm size range are important to atmospheric aerosol characterization (McMurry, 2000). Measurements aloft are especially important to understand aerosols in remote regions (Creamean et al., 2020; Herenz et al., 2018), and to mapping three-dimensional profiles (Mamali et al., 2018; Ortega et al., 2019; Zheng et al., 2021). Traditional mobility analyzers that span this size range are large, and not suitable for most unmanned aerial vehicle (UAV) or tethered balloon payloads that increasingly serve as the platform for aerosol characterization aloft. Moreover, aircraft measurements also require a fast scan time resolution to enable a good spatial resolution, as time is proportional to distance traveled in a moving platform.

To that end, Amanatidis et al. (2020) developed the "Spider DMA", a compact, lightweight, and fast differential mobility analyzer (DMA). The instrument was designed for 10–500 nm sizing, with an aerosol flowrate of 0.3 L/min to provide adequate

https://doi.org/10.5194/amt-2021-59
Preprint. Discussion started: 8 March 2021


Atmospheric Measurement Techniques Discussions

counting statistics on ambient aerosol over the time window appropriate for moving platforms. However, its compact size was achieved through reduction of mobility resolution; instead of the typical factor of 10 ratio between the sheath and aerosol flows, the Spider DMA employs a factor of 3. For given sample flowrate, obtaining higher resolution requires increasing the sheath flowrate, which in turn comes at the expense of dynamic sizing range; thus, a larger classifier would be required to maintain both sizing range and high resolution.

While high size resolution is important for specific applications, such as in laboratory calibrations that employ a DMA as a calibration aerosol source, it may not be critical for ambient size distribution measurements, wherein the particle distribution spans a much wider size range than the transfer function of the DMA. In addition to the smaller physical size for the instrument, operating at lower resolution increases the number of particle counts per size bin, and thus decreases the statistical uncertainty. This can be an important factor for low-concentration measurements.

The question explored in this paper is whether the moderate resolution mobility sizing of the Spider DMA is sufficient to capture the important characteristics of atmospheric aerosol size distributions. We begin with the derivation of the Spider DMA transfer function through a combination of finite element simulations and laboratory calibrations. We then present a field validation by comparison of ambient aerosol data from the new instrument with that obtained from a traditional long-column cylindrical DMA (LDMA) operated at a nominal resolution of $R = 10$ during nearly one month of continuous operation of the two, co-located instruments.

2 Methods

2.1 Spider DMA

The prototype Spider DMA sizing system consists of the "Spider" DMA (Amanatidis et al., 2020) and the "MAGIC" particle counter (Hering et al., 2014, 2019). The Spider is a compact mobility analyzer designed for applications requiring high portability and time resolution. It features a radial flow geometry and a sample inlet distribution system where the flow is azimuthally distributed through curved ("Spider"-like) flow channels. The instrument was designed to operate at 0.3 L/min sample, and 0.6–1.2 L/min sheath flowrates, offering size classification in the 10–500 nm size range. Owing to its small classification volume, the mean gas residence time in the classifier is on the order of ~ 1 s, making it possible to complete its voltage scan in times well below 60 s without significant smearing of its transfer function.

The "MAGIC" (Moderated Aerosol Growth with Internal water Cycling) particle counter is a laminar-flow water-based CPC. It employs a particle growth tube chamber with three stages (cool, warm, and cool) in which ultrafine particles grow by heterogeneous water vapor condensation to $> 1\,\mu\mathrm{m}$, and are subsequently counted by an optical detector. The final stage of the MAGIC CPC growth tube (moderator) recovers excess water vapor, enabling long-term operation without the need of a reservoir or water refilling. The instrument operates at a sample flowrate of 0.3 L/min, and has a 50% detection cut-point of $\sim$ 7 nm.

https://doi.org/10.5194/amt-2021-59
Preprint. Discussion started: 8 March 2021

Atmospheric Measurement Techniques Discussions

2.2 Transfer function determination by finite element modeling

Amanatidis et al. (2020) evaluated the Spider DMA transfer function in static-mode based on the Stolzenburg (1988) transfer function model and its derivation for radial flow classifiers (Zhang et al., 1995; Zhang and Flagan, 1996). Here, we evaluate its transfer function at "scanning" mobility mode, wherein the electric field is varied continuously in an exponential voltage ramp (Wang and Flagan, 1990). The scanning transfer function was evaluated with 2D finite element simulations of flows, quasi-steady-state electric field, and particle trajectories, using COMSOL Multiphysics. Simulations were performed for 0.9 / 0.3 L/min sheath / aerosol flowrates, scanning voltage in the range 5 – 5000V, and 30s exponential ramps for both up- and down-scans. Particles were modeled with the "Mathematical particle tracing" module, in which particle mass was assumed to be negligible since the electric field varies slowly, on a time scale that is long compared to the aerodynamic relaxation time of the particles being measured. Particle motion was calculated explicitly, by assigning particle velocity vector components equal to the steady-state fluid field solution, combined with the axial velocity acquired from interaction with the time-varying electrostatic field. Moreover, a Gaussian random-walk was employed in each time step of the solver to simulate particle Brownian motion, with a standard deviation proportional to particle diffusivity, i.e. $\mathrm{d}\sigma = \sqrt{2\,D\,\mathrm{d}t}$. Monodisperse particles were injected in regular intervals over the scan, varying from 0.025s for large particles to 0.003s for those in the diffusing size range. Modeling was repeated for 10 discrete particle sizes, spanning the dynamic range of the classifier.

2.3 Experimental

The two sizing instruments, the Spider DMA and the LDMA system, were operated in parallel, sampling ambient air from a roof top at the Caltech campus in Pasadena, CA. Measurements were made between May 16 - June 11, 2020, and were done as part of a study of the impacts of the COVID-19 pandemic shut-down on air quality.

The experimental setup used is shown in Figure 1. Ambient aerosol samples passed through a soft X-ray charge conditioner, and were subsequently split between the two mobility sizing systems. Both systems were operated in scanning mode. Both used a MAGIC water-based CPC as the detector. The size pre-cut stage in the inlet of both CPCs was removed to avoid additional smearing of the transfer functions. The Spider DMA was operated at 0.9 L/min sheath and 0.3 L/min aerosol flowrates. Its scanning program included a 30s upscan followed by a 30s downscan, during which the electrode voltage was exponentially varied between 5 – 5,000V. The voltage was held steady for an additional 2s at each end of the voltage ramp to allow for incoming particles to transmit through the classifier. Particle counts over the scan were recorded with a 5 Hz rate. The LDMA system was based on a TSI 3081 long-column DMA operated at 3.0 L/min sheath and 0.3 L/min aerosol flowrates, offering classification in the 17–989 nm size range. The scans consisted of an exponentially increasing (upscan) voltage ramp between 25–9,875V with a 330s duration. As with the Spider DMA, the LDMA voltage was held constant at the beginning and end of the ramp for 15s, bringing its duty cycle to 360s. Particle counts for the LDMA system were recorded with a 2 Hz sampling rate. Data acquisition and instrument control (flows, high voltage) was performed with custom LabVIEW software for both systems.

https://doi.org/10.5194/amt-2021-59
Preprint. Discussion started: 8 March 2021

Atmospheric Measurement Techniques Discussions

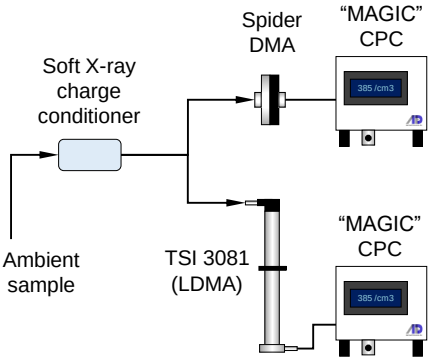

Figure 1. Schematic of the experimental setup used to evaluate the Spider DMA. The prototype instrument was operated at 0.9 L/min sheath and 0.3 L/min aerosol flowrates, and a scanning voltage program consisting of a 30s upscan followed by a 30s downscan. A TSI 3081 long-column DMA, operated at 3.0 L/min sheath and 0.3 L/min aerosol flows, 330s upscans, was used for comparison. Both sizing systems used an ADI "MAGIC" CPC as the particle detector.

2.4 Data inversion & analysis

Particle size distributions were obtained by inverting the raw particle counts recorded over each voltage scan. Raw counts were smoothed prior the inversion by Locally Weighted Scatterplot Smoothing (LOWESS) regression (Cleveland, 1979) to minimize inversion artefacts for noisy scans. The smoothed data were then inverted by employing regularized non-negative least squares minimization for both systems.

The inversion kernel for the Spider DMA system was based on the scanning transfer function of the Spider DMA obtained by finite element modeling. In order to generate a dense kernel required for the inversion, the modeled transfer function data were fitted in Gaussian distributions, whose parameters were subsequently fitted to analytical expressions that allowed generation of transfer functions at any instant (i.e., time bin) over the voltage scan. The Spider transfer functions were subsequently convoluted with a continuous stirred-tank reactor (CSTR) model (Russell et al., 1995; Collins et al., 2002; Mai et al., 2018) to take into account the time response of the MAGIC CPC. A 0.35s time-constant was used for the CSTR model in the Spider DMA system (Hering et al., 2017). The resulting transfer function was combined with a size-dependent transmission efficiency model described by Amanatidis et al. (2020) to take into account particle losses occurring at the Spider inlet, as those are not evaluated in the 2D finite element modeling. Raw counts were shifted to earlier time bins to account for the 1.50s plumbing time delay between the Spider outlet and the MAGIC CPC detector. Because the simulation enabled a strictly monodisperse "calibration" aerosol, the ratio of the number exiting the DMA during a particular counting time interval over the upstream particle number is the instrument transfer function.

The kernel for the LDMA system was based on the scanning transfer function model derived recently by Huang et al. (2020). A CSTR model with a characteristic time of 0.35s, and a plumbing delay time of 0.95s were used to incorporate the response

https://doi.org/10.5194/amt-2021-59
Preprint. Discussion started: 8 March 2021

Atmospheric Measurement Techniques Discussions

of the MAGIC CPC used in the LDMA system. The particle charge probability in the data inversion for both systems was assumed to follow the Wiedensohler approximation of the Boltzmann charge distribution (Wiedensohler, 1988).

3 Results

3.1 Spider scanning transfer function

Figure 2 shows the scanning transfer function of the Spider DMA evaluated by finite element modeling. Results are plotted as a function of time in the scan, for upscan and downscan voltage ramps. Each peak represents the ratio of particle number at the outlet over the inlet, for a specific input particle size. Finite element modeling data, shown with symbols, have been fitted to Gaussian distributions, shown with solid lines, which provide a close approximation to both upscan and downscan modeling data. As will be shown next, the Gaussian fits are subsequently employed to generate the transfer function at any time instance over the scan. Comparison between upscan and downscan peaks reveals a distinct difference; downscan peaks have a higher

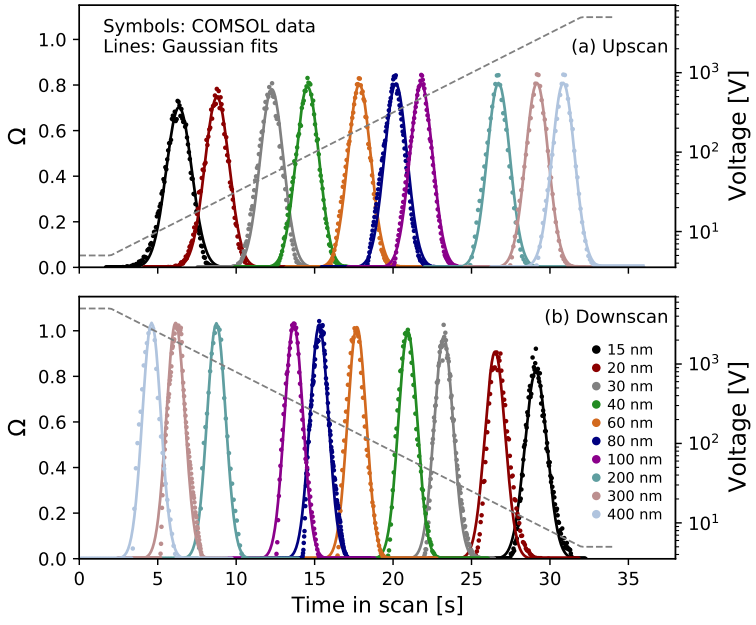

Figure 2. Finite element modeling of the Spider DMA scanning transfer function for (a) upscan and (b) downscan exponential voltage ramps with 30s duration, 0.9 L/min sheath and 0.3 L/min aerosol flowrates. Symbols correspond to finite element modeling data (ratio of particle number at the outlet over the inlet); solid lines show Gaussian distributions fitted to the modeling data; dashed lines indicate the scanning voltage program (values shown on right y-axis).

maximum number ratio. Moreover, they are somewhat narrower than the upscan peaks. This difference is the result of the scanning voltage operating mode. It should be noted that the transmission efficiency through the classification zone of a DMA is proportional to the area under the peak, rather than its maximum value. Hence, particle transmission over downscans is not

https://doi.org/10.5194/amt-2021-59
Preprint. Discussion started: 8 March 2021

Atmospheric Measurement Techniques Discussions

necessarily higher than upscans. Diffusional broadening of the transfer function becomes important in the low voltage region of each ramp, increasing the transfer function width as voltage decreases, though the broadening is less than would be seen with a higher resolution DMA (Flagan, 1999).

Figure 3 shows the integrated transfer function of the Spider DMA system for the same operating conditions as those used in the experiments. The voltage program, shown in Figure 3a, consists of a 2s hold time at 5V, followed by a 30s upscan up to 5000V, a 2s hold time at 5000V, and a 30s downscan to 5V. The classified particle size follows roughly the exponential increase and decrease of the voltage over the scan. The peaks shown in Figure 3b consist of the Gaussian approximation of the Spider transfer function shown in Figure 2, combined with the size and time response of the MAGIC CPC, and the size-dependent transmission efficiency in the Spider inlet (Amanatidis et al., 2020).

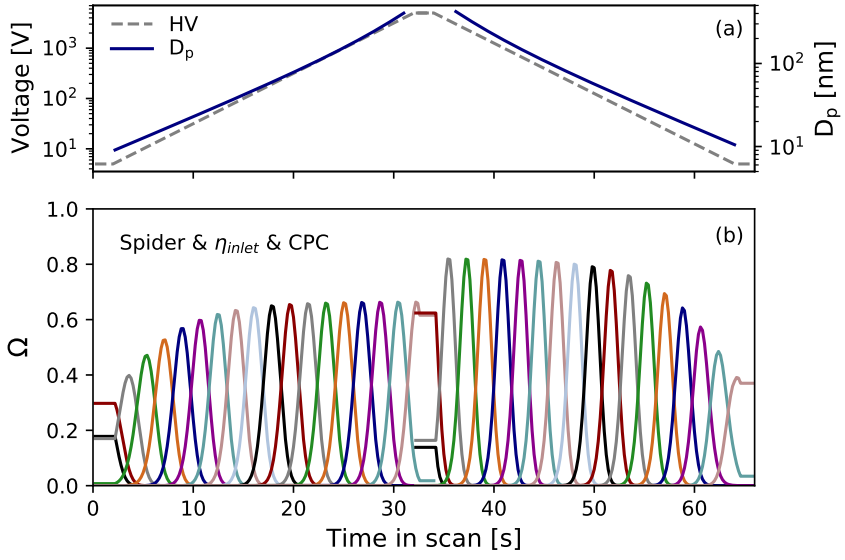

Figure 3. a) Scanning voltage and classified particle size over the Spider DMA scan. b) Transfer function of the integrated Spider DMA - MAGIC CPC system (ratio of particle number at the outlet over the inlet), consisting of the Spider DMA scanning transfer function combined with its inlet transmission efficiency and the MAGIC CPC response.

3.2 Data inversion example

Figure 4 demonstrates an inversion example for representative Spider DMA data. Particle raw counts recorded at each time bin over the upscan and downscan are shown in Figure 4a. Smooth lines are fitted to the raw counts data to minimize artefacts in the inversion process. The resulting size distributions, employing an inversion kernel based on the scanning transfer function in Figure 3b, are shown in Figure 4b. Up- and downscan distributions are almost identical in both shape and magnitude. The mean of the two distributions, as shown here, is used as the output of each scan.

https://doi.org/10.5194/amt-2021-59
Preprint. Discussion started: 8 March 2021

Atmospheric Measurement Techniques Discussions

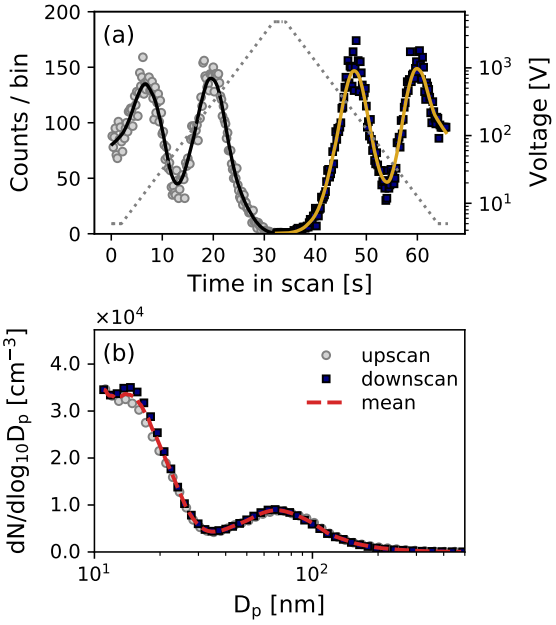

Figure 4. Example of Spider DMA data inversion. a) Raw counts per bin (symbols) recorded over the voltage ramp (up- and down-scan). Solid lines indicate LOWESS smoothing to the raw counts. b) Resulting size distributions after data inversion. The dashed line shows the mean of the up- and downscan distributions.

3.3 Instrument comparison

Figure 5 illustrates an excerpt of the Spider and LDMA size distribution measurements over a time period of 3 days. The two instruments report similar diurnal variation in the particle size distribution, in both size and number concentration. Increased particle concentrations were recorded in the early afternoon of each day, a regular occurrence as particles from morning traffic are transported by the sea breeze from Los Angeles to Pasadena where the measurements took place. Concentrations begin to drop later in the afternoon and through the evening, from about 15,000 cm^{-3} to below 5,000 cm^{-3}. The geometric mean diameter (GMD) of the size distribution ranged between about 30–60 nm, and was smaller over the high number concentration events recorded in early afternoon.

Figure 6 shows the evolution of the size distribution over a period of 2 hours in the afternoon of May 28, 2020 (indicated with dashed box in Figure 5d), measured with the Spider and the LDMA system. Since the measurement duty cycle of the two instruments was different (66s for the Spider vs 360s for the LDMA), we employed 30 min averaging of the recorded size distributions. This corresponds to 5 scans for the LDMA, and about 27 up- and down-scans for the Spider. The shaded areas of the averaged distributions represent the variation over the averaging period. Starting from a mono-modal distribution with a peak at ~ 45 nm (panel a), the size distribution transitioned to a bi-modal one over a period of 60 min (panels b, c), before transitioning back to a mono-modal distribution (panel d). As indicated by the shaded areas, there was high variation in the

https://doi.org/10.5194/amt-2021-59
Preprint. Discussion started: 8 March 2021

Atmospheric Measurement Techniques Discussions

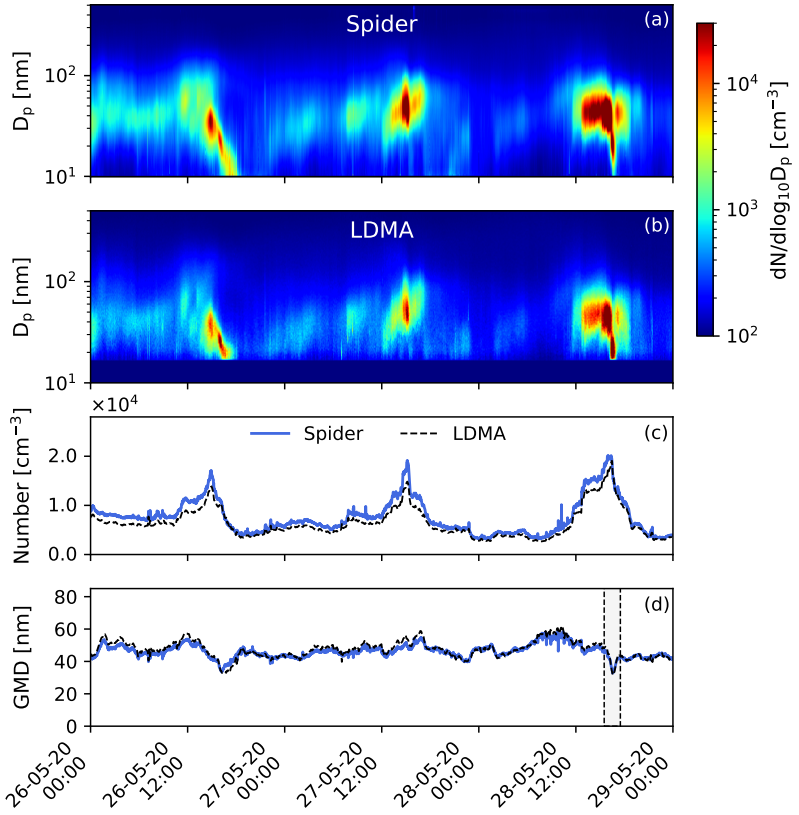

Figure 5. Evolution of the particle size distribution over a period of 3 days measured by a) the Spider DMA, and b) the LDMA system. Corresponding total particle number and geometric mean diameter, calculated over the 17–500 nm size range, are shown in panels (c) and (d), respectively. Solid blue color in panel (b) (size range <17nm) was used for no available data in the LDMA system. The dashed box in panel (d) indicates the time period shown in Figure 6.

aerosol concentration during this transition event. Overall, the measurement of the two instruments was in good agreement both in terms of sizing and concentration, suggesting that the lower sizing resolution in the Spider DMA was adequate in capturing the details of the size distribution. An animation video with side-by-side comparison of 30-min averaged distributions for the entire testing period is included in the Supplementary Material (Amanatidis et al., 2021).

Figure 7 compares the total number and geometric mean diameter measured by the two instruments over the entire testing period. Each data point corresponds to a 1-hour average of the size distribution measured by each instrument, calculated over the 17–500 nm size range where the two systems overlap. Overall, the comparison includes 550h of measurement data. In order to identify outliers in the data, we employed the "RANSCAC" (random sample consensus) algorithm (Fischler and Bolles, 1981). In this, random samples of the data are selected, analyzed, and classified as inliers and outliers through an iterative routine. The outliers identified are shown in Figure 7 with open square symbols.

https://doi.org/10.5194/amt-2021-59
Preprint. Discussion started: 8 March 2021

Atmospheric Measurement Techniques Discussions

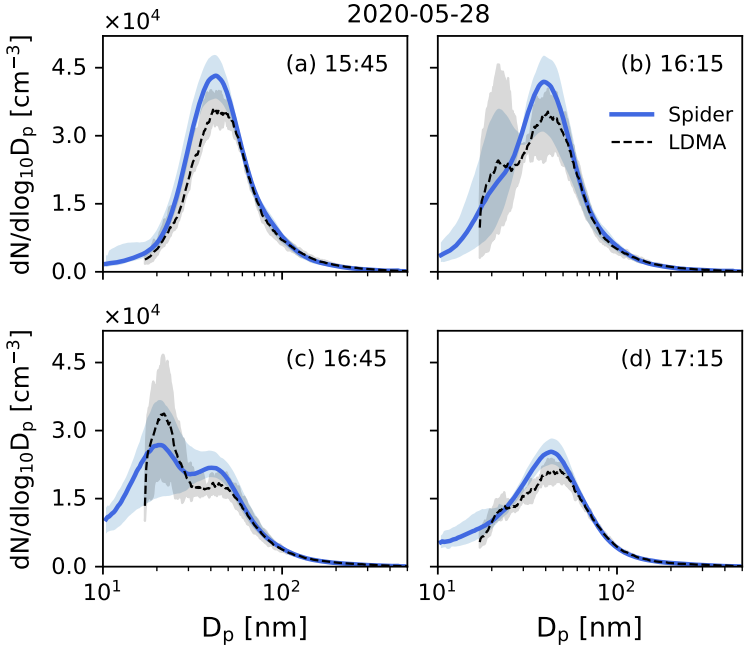

Figure 6. Evolution of the size distribution in the afternoon of May 28, 2020, as measured by the Spider and LDMA systems. Lines represent the mean of size distributions measured over a period of 30 min. Shaded areas demonstrate the variation of the size distribution over the averaging period, indicating maximum and minimum values.

Next, a linear regression model (no intercept) was fitted to the data (excluding outliers) to evaluate the correlation between the two instruments. Since both instruments include measurement errors, we employed Orthogonal Distance Regression (Boggs et al., 1987), where errors on both the dependent and independent variable are taken into account in the least squares minimization. The resulting regression lines exhibit slopes of $\alpha = 1.13$ and $\alpha = 1.00$ for number concentration and GMD, respectively, suggesting an overall excellent agreement between the instruments. Moreover, Pearson correlation coefficients of $\rho = 0.98$ and $\rho = 0.93$ indicate a strong correlation for both metrics of the size distribution.

3.4 Operational observations

The prototype Spider DMA used in this study incorporated an electrostatic-dissipative plastic that failed after several months of continuous operation, causing arcing within the instrument at the highest voltages. The Spider DMA has been redesigned to eliminate this material, and is currently being tested. This new Spider DMA has relatively minor changes to the classification region of the prototype presented here, and employs the same moderate resolution approach to maintain a compact size.

https://doi.org/10.5194/amt-2021-59
Preprint. Discussion started: 8 March 2021

Atmospheric Measurement Techniques Discussions

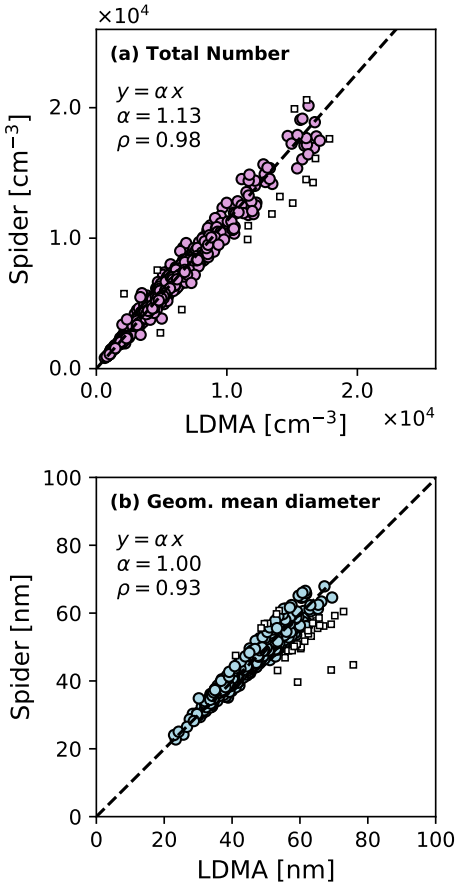

Figure 7. Comparison of a) total particle number, and b) geometric mean diameter, measured by the Spider and LDMA systems over a period of 26 days of continuous testing. Each point represents 1 hour averaged data, calculated over the 17–500 nm size range where the two instruments overlap. Square symbols show outliers excluded from the regression analysis. Dashed lines represent a linear regression model (no intercept) fitted to the data. ρ values denote the Pearson correlation coefficient between the measurement data of the two instruments.

https://doi.org/10.5194/amt-2021-59
Preprint. Discussion started: 8 March 2021

Atmospheric Measurement Techniques Discussions

4 Summary & conclusions

We evaluated the performance of the Spider DMA, a highly-portable particle sizer, in measuring ambient size distributions against a co-located particle sizer based on a TSI 3081 long-column DMA (LDMA). Comparison measurements were performed at the Caltech campus in Pasadena, CA over a period of 26 days, between May 16 – June 11, 2020, as part of a field campaign examining the effects of COVID-19 shut-down on air quality. The Spider DMA system was operated at a lower nominal sizing resolution (0.9 L/min sheath and 0.3 L/min aerosol flowrates, $R = 3$) than the LDMA (3.0 L/min sheath and 0.3 L/min aerosol flowrates, $R = 10$), and at a higher time resolution (30s vs 330s scans).

The transfer function of the Spider DMA was obtained by finite element modeling at the conditions employed in the experiment, which included both up- and downscan exponential voltage ramps with 30s duration. Modeling data were fitted to Gaussian distributions, and were combined with the experimentally-determined transmission efficiency of the Spider DMA and the MAGIC particle counter response function to generate the inversion kernel of the combined system. Data inversion of the LDMA system was based on the semi-analytical model of the LDMA scanning transfer function derived by Huang et al. (2020).

Regression analysis of 550h of measurement data showed an overall excellent correlation between the two instruments, with slopes of $\alpha = 1.13$ and $\alpha = 1.00$, and Pearson correlation coefficients of $\rho = 0.98$ and $\rho = 0.93$ in the reported particle number and geometric mean diameter (GMD), respectively. The good agreement between the two instruments suggests that particle sizers operated at moderate resolution ($R = 3$ in this study) can sufficiently capture the dynamics and key characteristics of ambient size distributions, at least in the 10–500 nm size range. Lowering the resolution enables a wider dynamic range, or a more compact particle sizer for a desired size range, which is essential in many field applications, such as for measurements aloft with small UAVs or tethered balloons that have limited payloads. Moreover, it enables better counting statistics, as the wider transfer function results in higher counts per size bin, which is an important factor at low concentration aerosol measurements.

Author contributions. SA performed the finite element modeling for the Spider DMA instrument, analyzed its measurement data, generated the figures, and wrote the manuscript text. YH analyzed the LDMA instrument data and prepared the experimental setup. BP, BCS, CMK and RXW collected the measurement data and provided technical maintenance to the instruments. JHS reviewed and provided editorial feedback on the manuscript. SVH and RCF planned the experiments, and contributed to results interpretation and editing of the manuscript.

Competing interests. RCF and SA are inventors of the "Spider" DMA technology patent (US10775290B2) which is licensed to SVH's company. The rest of the authors declare that they have no conflict of interest.

Disclaimer. Neither the United States Government nor any agency thereof, nor any of their employees, makes any warranty, express or implied, or assumes any legal liability or responsibility for the accuracy, completeness, or usefulness of any information, apparatus, product,

https://doi.org/10.5194/amt-2021-59
Preprint. Discussion started: 8 March 2021

or process disclosed, or represents that its use would not infringe privately owned rights. Reference herein to any specific commercial
200 product, process, or service by trade name, trademark, manufacturer, or otherwise does not necessarily constitute or imply its endorsement, recommendation, or favoring by the United States Government or any agency thereof. The views and opinions of authors expressed herein do not necessarily state or reflect those of the United States Government or any agency thereof.

Acknowledgements. The authors gratefully acknowledge support by the U.S. Department of Energy, Office of Science, under Award Number(s) DE-SC0013152, by the Department of Health and Human Services, Centers for Disease Control and Prevention under Award OH010515

https://doi.org/10.5194/amt-2021-59
Preprint. Discussion started: 8 March 2021

Atmospheric Measurement Techniques Discussions

References

Amanatidis, S., Kim, C., Spielman, S. R., Lewis, G. S., Hering, S. V., and Flagan, R. C.: The Spider DMA: A miniature radial differential mobility analyzer, Aerosol Science and Technology, https://doi.org/10.1080/02786826.2019.1626974, 2020.

Amanatidis, S., Huang, Y., Pushpawela, B., Schulze, B. C., Kenseth, C. M., Ward, R. X., Seinfeld, J. H., Hering, S. V., and Flagan, R. C.: Efficacy of a portable, moderate-resolution, fast-scanning DMA for ambient aerosol size distribution measurements, https://doi.org/10.22002/D1.1896, https://data.caltech.edu/records/1896, 2021.

Boggs, P. T., Byrd, R. H., and Schnabel, R. B.: A Stable and Efficient Algorithm for Nonlinear Orthogonal Distance Regression, SIAM Journal on Scientific and Statistical Computing, 8, 1052–1078, https://doi.org/10.1137/0908085, http://epubs.siam.org/doi/10.1137/0908085, 1987.

Cleveland, W. S.: Robust Locally Weighted Regression and Smoothing Scatterplots, Journal of the American Statistical Association, 74, 829–836, https://doi.org/10.1080/01621459.1979.10481038, https://www.tandfonline.com/doi/abs/10.1080/01621459.1979.10481038, 1979.

Collins, D. R., Flagan, R. C., and Seinfeld, J. H.: Improved inversion of scanning DMA data, Aerosol Science and Technology, 36, 1–9, https://doi.org/10.1080/027868202753339032, 2002.

Creamean, J., de Boer, G., Telg, H., Mei, F., Dexheimer, D., Shupe, M., Solomon, A., and McComiskey, A.: Assessing the vertical structure of Arctic aerosols using tethered-balloon-borne measurements, Atmospheric Chemistry and Physics, 21, 1–34, https://doi.org/10.5194/acp-2020-989, https://acp.copernicus.org/articles/21/1737/2021/, 2020.

Fischler, M. A. and Bolles, R. C.: Random sample consensus, Communications of the ACM, 24, 381–395, https://doi.org/10.1145/358669.358692, https://dl.acm.org/doi/10.1145/358669.358692, 1981.

Flagan, R. C.: On Differential Mobility Analyzer Resolution, Aerosol Science and Technology, 30, 556–570, https://doi.org/10.1080/027868299304417, http://www.tandfonline.com/doi/abs/10.1080/027868299304417, 1999.

Herenz, P., Wex, H., Henning, S., Bjerring Kristensen, T., Rubach, F., Roth, A., Borrmann, S., Bozem, H., Schulz, H., and Stratmann, F.: Measurements of aerosol and CCN properties in the Mackenzie River delta (Canadian Arctic) during spring-summer transition in May 2014, Atmospheric Chemistry and Physics, https://doi.org/10.5194/acp-18-4477-2018, 2018.

Hering, S. V., Spielman, S. R., and Lewis, G. S.: Moderated, Water-Based, Condensational Particle Growth in a Laminar Flow, Aerosol Science and Technology, 48, 401–408, https://doi.org/10.1080/02786826.2014.881460, http://www.tandfonline.com/doi/abs/10.1080/02786826.2014.881460, 2014.

Hering, S. V., Lewis, G. S., Spielman, S. R., Eiguren-Fernandez, A., Kreisberg, N. M., Kuang, C., and Attoui, M.: Detection near 1-nm with a laminar-flow, water-based condensation particle counter, Aerosol Science and Technology, 51, 354–362, https://doi.org/10.1080/02786826.2016.1262531, http://dx.doi.org/10.1080/02786826.2016.1262531, 2017.

Hering, S. V., Lewis, G. S., Spielman, S. R., and Eiguren-Fernandez, A.: A MAGIC concept for self-sustained, water-based, ultrafine particle counting, Aerosol Science and Technology, 53, 63–72, https://doi.org/10.1080/02786826.2018.1538549, https://www.tandfonline.com/doi/full/10.1080/02786826.2018.1538549, 2019.

Huang, Y., Seinfeld, J. H., and Flagan, R. C.: Diffusional Transfer Function for the Scanning Electrical Mobility Spectrometer (SEMS), Aerosol Science and Technology, 6826, 1–24, https://doi.org/10.1080/02786826.2020.1760199, https://www.tandfonline.com/doi/full/10.1080/02786826.2020.1760199, 2020.

https://doi.org/10.5194/amt-2021-59
Preprint. Discussion started: 8 March 2021

Atmospheric Measurement Techniques Discussions

Mai, H., Kong, W., Seinfeld, J. H., and Flagan, R. C.: Scanning DMA Data Analysis II. Integrated DMA-CPC Instrument Response and Data Inversion, Aerosol Science and Technology, 52, 1–35, https://doi.org/10.1080/02786826.2018.1528006, https://www.tandfonline.com/doi/full/10.1080/02786826.2018.1528006, 2018.

Mamali, D., Marinou, E., Sciare, J., Pikridas, M., Kokkalis, P., Kottas, M., Binietoglou, I., Tsekeri, A., Keleshis, C., Engelmann, R., Baars, H., Ansmann, A., Amiridis, V., Russchenberg, H., and Biskos, G.: Vertical profiles of aerosol mass concentration derived by unmanned airborne in situ and remote sensing instruments during dust events, Atmospheric Measurement Techniques, https://doi.org/10.5194/amt-11-2897-2018, 2018.

McMurry, P. H.: A review of atmospheric aerosol measurements, Atmospheric Environment, https://doi.org/10.1016/S1352-2310(99)00455-0, 2000.

Ortega, J., Snider, J. R., Smith, J. N., and Reeves, J. M.: Comparison of aerosol measurement systems during the 2016 airborne ARISTO campaign, Aerosol Science and Technology, https://doi.org/10.1080/02786826.2019.1610554, 2019.

Russell, L. M., Flagan, R. C., and Seinfeld, J. H.: Asymmetric instrument response resulting from mixing effects in accelerated DMA-CPC measurements, Aerosol Science and Technology, 23, 491–509, https://doi.org/10.1080/02786829508965332, 1995.

Stolzenburg, M. R.: An ultrafine aerosol size distribution measuring system, Doctoral dissertation, University of Minnesota, 1988.

Wang, S. C. and Flagan, R. C.: Scanning electrical mobility spectrometer, Aerosol Science and Technology, 13, 230–240, https://doi.org/10.1080/02786829008959441, 1990.

Wiedensohler, A.: An approximation of the bipolar charge distribution for particles in the submicron size range, Journal of Aerosol Science, https://doi.org/10.1016/0021-8502(88)90278-9, 1988.

Zhang, S.-H. and Flagan, R. C.: Resolution of the radial differential mobility analyzer for ultrafine particles, Journal of Aerosol Science, 27, 1179–1200, https://doi.org/10.1016/0021-8502(96)00036-5, http://linkinghub.elsevier.com/retrieve/pii/0021850296000365https://linkinghub.elsevier.com/retrieve/pii/0021850296000365, 1996.

Zhang, S.-H., Akutsu, Y., Russell, L. M., Flagan, R. C., and Seinfeld, J. H.: Radial Differential Mobility Analyzer, Aerosol Science and Technology, 23, 357–372, https://doi.org/10.1080/02786829508965320, http://www.tandfonline.com/doi/abs/10.1080/02786829508965320, 1995.

Zheng, G., Wang, Y., Wood, R., Jensen, M. P., Kuang, C., McCoy, I. L., Matthews, A., Mei, F., Tomlinson, J. M., Shilling, J. E., Zawadowicz, M. A., Crosbie, E., Moore, R., Ziemba, L., Andreae, M. O., and Wang, J.: New particle formation in the remote marine boundary layer, Nature Communications, https://doi.org/10.1038/s41467-020-20773-1, 2021.